Bremsstrahlung Emission of an X -Band Permanent Magnet Minimum-B Quadrupole Electron Cyclotron Resonance Ion Source

Olli Tarvainen, Ville Toivanen, Taneli Kalvas, Hannu A. Koivisto, Sami Kosonen

Bremsstrahlung Emission of an X-Band Permanent Magnet Minimum-B Quadrupole Electron Cyclotron Resonance Ion Source

Olli Tarvainen, Ville Toivanen, Taneli Kalvas, Hannu Koivisto and Sami Kosonen

Abstract—We have carried out bremsstrahlung measurements on a permanent magnet minimum-B quadrupole Electron Cyclotron Resonance (ECR) ion source operating at 10.3–11.5 GHz microwave frequencies. The bremsstrahlung spectral temperature is found at 30–35 keV in a wide ranges of microwave power, frequency and neutral gas feed rate. The result implies that the B_{min}-scaling of the spectral temperature, observed for conventional ECR ion sources, is a fundamental property of the electron heating in minimum-B devices, not specific to the field topology. Similar to conventional ECR ion sources, the bremsstrahlung count rate increases linearly with the microwave power but does not depend on the neutral gas pressure. It is demonstrated that dual frequency heating can improve the beam currents of high charge state argon ion beams and reduce the bremsstrahlung emission. Plasma breakdown and decay transient measurements of the bremsstrahlung power flux indicate that the electron confinement in the quadrupole field is weaker than in conventional ECR ion sources using a superposition of solenoid and sextupole fields.

Index Terms—Electron Cyclotron Resonance (ECR) Plasma, Bremsstrahlung, Ion sources

I. INTRODUCTION

THE high charge state ion beam production with minimum-B Electron Cyclotron Resonance Ion Sources (ECRIS) has made order-of-magnitude performance leaps since their early development in 1970's [1]. The overarching guideline behind the advances has been the realization that ECRIS plasma density and the beam currents of the most prevalent charge states scale with the square of the microwave frequency, i.e. $n_e \propto f_{RF}^2$ or $I_{peak} \propto f_{RF}^2$. Thus, ECR ion sources are often catalogued to 1st–4th generation sources depending on the microwave frequency applied for the plasma (electron) heating. The ECRIS generations, their microwave bands and selected examples of ion sources are summarised in Table I.

The availability of high frequency microwave amplifiers has never posed a limitation to ECRIS development. Instead, it is the technology required for generating the necessary minimum-B magnetic structure, namely the combination of solenoid and sextupole fields, that has defined the pace of progress over the past decades. It has been found that in

O. Tarvainen is with the UK Research and Innovation, STFC Rutherford Appleton Laboratory, ISIS Pulsed Spallation Neutron and Muon Facility, Harwell Campus, OX11 0QX, United Kingdom

V. Toivanen, T. Kalvas, H. Koivisto and S. Kosonen are with the Accelerator Laboratory, Department of Physics, University of Jyväskylä, FIN-40014 Jyväskylä, Finland

e-mail: olli.tarvainen@stfc.ac.uk

Manuscript received XXX, 2023; revised XXX, 2023.

the high-B operation mode [11] the peak solenoid field should be approximately 4 times and radial (sextupole) field 2 times the cold electron resonance field B_{ECR} [12] with $B_{ECR}[T] = f[GHz]/28$. The magnetic field scaling implies that the highest practical frequency for room-temperature ion sources with electromagnet coils and permanent magnet sextupole is $18-20$ GHz, while 56 GHz is the highest conceivable microwave frequency with state-of-the-art Nb_3Sn superconducting coils [13].

Further increase in frequency and magnetic field requires alternative field topologies used e.g. in the 60 GHz SEISM cusp-source [14] or in the gasdynamic simple mirror SMIS source [15], which have not been optimised for very high charge state ion production. A very appealing option is to adopt the minimum-B quadrupole topology, produced by a "combined function coil" and used in mirror confinement fusion plasma research [16], [17], [18], demonstrating the existence of high charge state ions up to Ar^{11+} but never optimised for beam formation. A relatively recent design study [19] has demonstrated the feasibility of a superconducting (Nb_3Sn) minimum-B quadrupole "ARC-ECRIS", consisting of a single coil with several layers of superconducting wire loops and allowing 100 GHz operation with adequate mirror ratios, which could be a game-changer in surpassing the limitations of conventional ECR ion sources. The JYFL (University of Jyväskylä, Department of Physics) ion source group has developed two room-temperature prototype ion sources utilizing the minimum-B quadrupole field topology. The first 6.4 GHz proof-of-concept electromagnet ARC-ECRIS demonstrated the production of argon ion beams up to charge state Ar^{6+} [20]. The second prototype source, the CUBE-ECRIS, is a permanent magnet device operating at X-band microwave frequencies from 10 to 11.5 GHz, and has demonstrated charge states Ar^{12+}, Kr^{19+} and Xe^{24+} with >5 µA of Ar^{10+}, for example [21]. These ion sources (ARC-ECRIS and CUBE-ECRIS) have rather similar field topology as the Quadrumafios source developed in Grenoble at 1990's [22], the main difference being the simplified magnet configuration. The ARC and CUBE sources utilize either a combined function electromagnet or permanent magnet array instead of separate solenoid and quadrupole magnets used for the Quadrumafios source. The latter was built for dedicated plasma diagnostics experiments and demonstrated argon ion beams up to charge state Ar^{11+} ($1-2$ µA with 2 kW microwave power at 10 GHz) [22].

One challenge in developing ECR ion sources with alter-

TABLE I
CONVENTIONAL MINIMUM-B ECR ION SOURCE GENERATIONS, FREQUENCY BANDS AND EXAMPLES OF ION SOURCES.

ECRIS generation	Frequency range [GHz]	Amplifier technology (typical)	Example ion source(s)	Conductor type
1st	6.4–8	C-band klystron	LBNL ECR [2]	Room-temp.
2nd	10–14.5	X- or Ku-band klystron or TWT	Caprice [3] / LBNL A-ECR [4]	Room-temp.
2.5th	18–20	Ku-band klystron	HIISI [5] / SuSI [6]	Room-temp. / Supercon.
3rd	24–28	K- or Ka-band gyrotron	VENUS [7] / SECRAL II [8]	Supercon.
4th or next gen. (future)	36–45	Q-band gyrotron	FECR [9] / MARS-D [10]	Supercon.

native magnetic field topologies, such as the CUBE-ECRIS, is the lack of knowledge on the importance of the required field parameters. The B-field scaling laws of the injetion, extraction, minimum and radial fields [12] for conventional, i.e. solenoid + sextupole -based sources, are well established, which is not the case for the quadrupole topology. The design of the permanent magnet CUBE-ECRIS was made for $10\,\mathrm{GHz}$ frequency [23] with the intention to reach the mirror ratios stipulated by the scaling laws of conventional ECR ion sources. It has later been found experimentally that the optimum operating frequency of the CUBE-ECRIS is $\sim11\,\mathrm{GHz}$ instead, which is presumably due to a trade-off between higher plasma density and larger plasma volume at higher frequency vs. lower mirror ratio $R = B_\mathrm{wall}/B_\mathrm{ECR}$ towards the chamber walls. Addressing the question of the magnetic field scaling in the minimum-B quadrupole topology requires diagnostics beyond the measurement of the extracted beam currents.

Bremsstrahlung diagnostic is a well-established method to probe the hot electron physics of ECR ion sources. For a general description of the method we refer the reader to a recent review [24] and the references therein. Thick target (wall) and plasma bremsstrahlung measurements conducted on conventional ECR ion sources have revealed a number of trends regarding the effect of the main tuning parameters of the ion source. Those, most relevant for the current paper, can be summarized as: (i) The total count rate (or plasma emissivity density) increases with the microwave power (see e.g. Ref. [25]). (ii) The magnetic field strength affects the high energy tail of the bremsstrahlung spectrum, most importantly it is the absolute value of the minimum-B (not $B_\mathrm{min}/B_\mathrm{ECR}$, B_inj, B_ext or B_rad or f_RF) that determines the bremsstrahlung spectral temperature [26]. (iii) The gas feed rate or plasma chamber pressure has very little effect on the bremsstrahlung emission (see e.g. Ref. [25]). (iv) There is a difference between the axially and radially emitted bremsstrahlung spectrum (not just the count rate), which is presumably due to the anisotropy of the electron velocity distribution ($v_\perp >> v_\parallel$) and the directionality of the photon emission [27], [25], [24]. While the end-point energy of the bremsstahlung spectrum reveals the maximum electron energy in the ECR discharge, it has thus far proven impossible to infer the electron energy distribution from the bremsstrahlung measurements.

In this paper we report the results of bremsstrahlung measurements taken on the CUBE-ECRIS. The motivation for the experiments is twofold. First, we want to understand if the bremsstrahlung spectrum could explain why the CUBE-

ECRIS works best (in terms of high charge state production) at frequencies of $\sim11\,\mathrm{GHz}$ especially in dual frequency heating mode [28], and what limits the range of frequencies where high charge state ion beams are effectively produced. Second, we want to compare the effects of the CUBE-ECRIS tuning parameters on the bremsstrahlung characteristics to those found in conventional ECR ion sources. The latter is an essential step for the potential development of super-conducting minimum-B quadrupole sources (e.g. the afore-mentioned $100\,\mathrm{GHz}$ ARC-ECRIS) for which the knowledge on bremsstahlung emission, i.e. maximum photon energy and spectral characteristics, is very limited but at the same time essential in terms of cryostat (heat load) and radiation shielding design.

II. THE CUBE-ECR ION SOURCE

The design of the permanent magnet CUBE-ECRIS is described in Ref. [23] presenting the detailed magnet design, plasma chamber dimensions, extraction and low energy beam transport. The technical details of the prototype ion source are discussed in the supplementary material of Ref. [29]. Here we recount the main features of the ion source and its magnetic field, relevant for this study.

The microwave radiation is launched into the CUBE-ECRIS through a WR75-waveguide port and the ion beam is extracted through a $4\,\mathrm{mm}$ by $40\,\mathrm{mm}$ slit. The fundamental difference between the CUBE-ERCIS and any other permanent magnet ECR ion source is the magnetic field topology. The CUBE-ECRIS uses a minimum-B quadrupole field with the plasma loss pattern towards the extraction forming a line instead of the conventional triangular pattern, which favors a slit extraction. Figure 1 shows the (simulated) total magnetic field B_tot of the CUBE-ECRIS along the axes passing through the minimum-B at ($x = y = z = 0\,\mathrm{mm}$). The location of the extraction electrode (slit) at $x = 92\,\mathrm{mm}$ and the cold electron resonance fields of $0.368\,\mathrm{T}$ and $0.411\,\mathrm{T}$ corresponding to $10.3\,\mathrm{GHz}$ and $11.5\,\mathrm{GHz}$, respectively, are indicated. These frequencies correspond to the extremes of the range used in our experiments. The simulated field has been experimentally verified as reported in Ref. [30].

The field topology is illustrated further in Fig. 2 showing the density and vector plots of the magnetic field in one quadrant/half of the structure. The complete field map can be obtained by mirroring the field about each symmetry plane. The closed ECR-surfaces at $0.368\,\mathrm{T}$ and $0.411\,\mathrm{T}$ correspond-ing to $10.3\,\mathrm{GHz}$ and $11.5\,\mathrm{GHz}$ frequencies are indicated with the solid lines (the inner one corresponding to $10.3\,\mathrm{GHz}$).
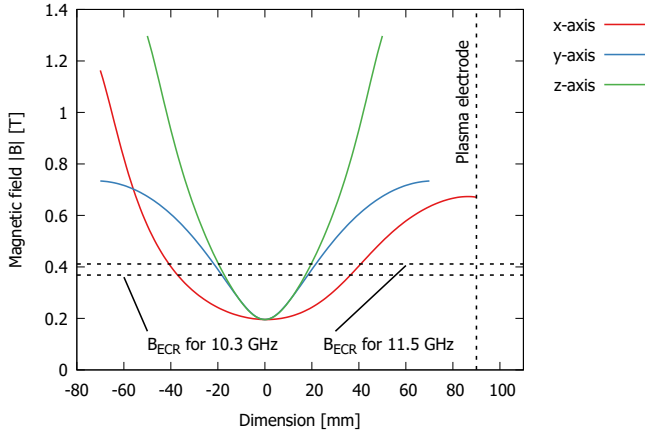
Fig. 1. The (total) magnetic field of the CUBE-ECR ion source on axes passing thorugh the minimum-B. The beam is extracted towards the positive x-coordinate with the plasma electrode (slit) position indicated in the figure. The horizontal dashed lines depict the resonance fields of $0.368\,\text{T}$ and $0.411\,\text{T}$ for $10.3\,\text{GHz}$ and $11.5\,\text{GHz}$ frequencies.

Table II lists the magnetic field parameters, i.e. relevant field values, mirror ratios $R = B_{\text{wall}}/B_{\text{ECR}}$ towards the field maxima, ECR-surface area S_{ECR}, volume V_{ECR} enclosed by the ECR-surface, and the average magnetic field gradient parallel to the field $\left\langle |(\vec{B}/|\vec{B}|) \cdot \nabla \vec{B}| \right\rangle$ on the ECR surface. The values are given for $10.3\,\text{GHz}$ and $11.5\,\text{GHz}$ frequencies marking the frequency range used in the bremsstrahlung measurements. The magnetic field parameters vary monotonically with the frequency, i.e. the given values represent the minima/maxima encountered in this study. The last closed magnetic isosurface is defined by the extraction field.

TABLE II
CUBE-ECRIS MAGNETIC FIELD PARAMETERS FOR $10.3 - 11.5\,\text{GHz}$ FREQUENCY RANGE.

B_{max} at $-x$ (back wall)	$1.04\,\text{T}$
B_{max} at $+x$ (extraction)	$0.67\,\text{T}$
B_{max} at $\pm y$ (wall, horizontal coordinate)	$0.73\,\text{T}$
B_{max} at $\pm z$ (wall, vertical coordinate)	$1.10\,\text{T}$
B_{min}	$0.21\,\text{T}$
B_{ECR}	$0.368 - 0.411\,\text{T}$
$B_{\text{min}}/B_{\text{ECR}}$	0.57–0.51
R towards $-x$ (back wall)	$2.83 - 2.53$
R towards $+x$ (extraction)	$1.82 - 1.63$
R towards $\pm y$ (wall, horizontal coordinate)	$1.98 - 1.78$
R towards $\pm z$ (wall, vertical coordinate)	$2.99 - 2.68$
S_{ECR}	$74 - 96\,\text{cm}^2$
V_{ECR}	$51 - 78\,\text{cm}^3$
$\left\langle |(\vec{B}/|\vec{B}|) \cdot \nabla \vec{B}| \right\rangle$ on the ECR surface	$6.58 - 7.10\,\text{T/m}$

It has been shown previously that despite of the different magnetic field topology, the CUBE-ECRIS works as one would expect a high charge state ECR ion source to do; it heats electrons to several hundred keV energies, produces beams of high charge state ions and exhibits an afterglow transient peak of the beam current implying electrostatic confinement as first reported in Ref. [29].

III. EXPERIMENTAL SETUP AND PROCEDURE

The main components of the experimental setup are presented in the schematic of the CUBE-ECRIS test stand in Fig. 3. The main components are the CUBE-ECRIS ion source, the adjacent beam line with an electrostatic quadrupole doublet for asymmetric focusing and steering, $102°$ dipole magnet for m/q-separation of the extracted beams and a downstream Faraday cup for beam current measurement.

Two types of x-ray detectors placed as shown in Fig. 3 were used for the bremsstrahlung measurement. The energy resolved bremsstrahlung spectra were recorded with an Amptek XR-100-CdTe x-ray detector placed behind a $30\,\text{mm}$ long lead collimator with a $3\,\text{mm}$ aperture. The detector was measuring the plasma bremsstrahlung and the thick-target bremsstrahlung emitted by the electrons interacting with the aluminium plasma electrode. The attenuation in the plasma electrode and surrounding mechanical structures renders the spectrum at gamma energies of $\leq 30\,\text{keV}$ unusable for analysis. The efficiency and energy calibration of the bremsstrahlung spectra is based on characteristic peaks of ^{241}Am and ^{133}Ba. The data acquisition time of the spectrum was set to $1200\,\text{s}$ ($20\,\text{min}$) to collect appropriate statistics at all ion source settings. The dead time of the detector was $\leq 8\%$ in all measurements, and is taken into account when comparing the bremsstrahlung count rates in Section IV. Pile-up events were automatically vetoed by the data acquisition system to avoid artificially inflating the high energy tail of the spectrum. The temporal evolution of the bremsstrahlung power flux with pulsed microwave injection was measured with a bismuth germanate x-ray scintillator coupled with a Na-doped CsI current-mode (DC-coupled) photomultiplier tube, placed in the same location as the energy-resolving x-ray detector. The scintillator signal is proportional to both, the energy of the emitted photons and their flux, i.e. the time-resolved signal is proportional to the bremsstrahlung power flux. The current signal of the photomultiplier was converted to a voltage signal with a transimpedance amplifier (Stanford Research Systems SR570) and recorded with an oscilloscope. The use of the scintillator allows measuring the breakdown and decay transient of the bremsstrahlung power flux at better than $10\,\mu\text{s}$ temporal resolution.

The bremsstrahlung spectra are characterized by two measures, the total count rate and spectral temperature. The total count rate is taken as the number of recorded counts divided by the measurement time (corrected by the dead time of the detector). The spectral temperature is calculated with a standard procedure, described e.g. in Ref. [26]. We first take the natural logarithm of the data in $60 - 160\,\text{keV}$ energy range, make a linear fit $\ln(\text{data}) = aE_\gamma + b$, and finally calculate the spectral temperature from the slope of the fit, i.e. $T_s = -1/a$.

There are several factors affecting the uncertainty related to the bremsstrahlung measurements and the spectral temperatures derived from the data. (i) Firstly, there is the question of repeatability, which was addressed by measuring the bremsstrahlung spectra multiple times at certain "standard" settings ($290\,\text{W}$ microwave power at $10.97\,\text{GHz}$) of the ion source. The count rate was observed to be identical within $\pm 1\%$ between these consecutive data acquisitions ($N = 6$)
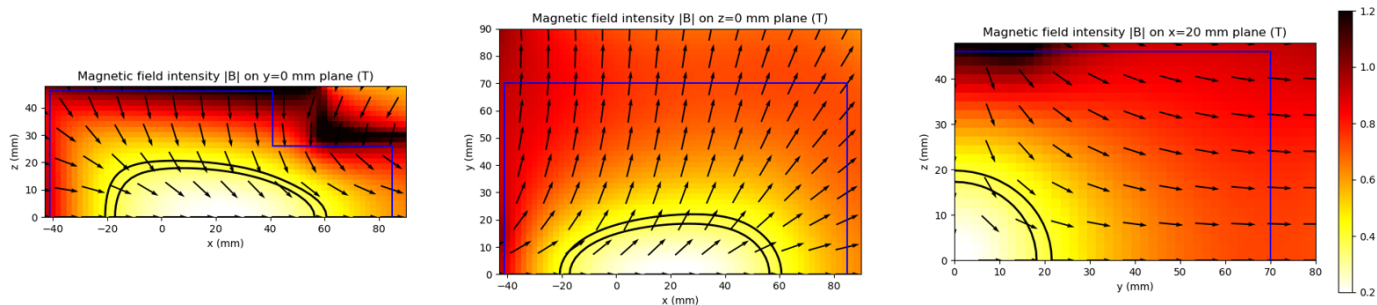
Fig. 2. The magnetic field density plot of the CUBE-ECRIS in different symmetry planes. The solid lines represent the closed surfaces with $0.368\,\mathrm{T}$ and $0.411\,\mathrm{T}$ magnetic field corresponding to $10.3\,\mathrm{GHz}$ and $11.5\,\mathrm{GHz}$ (cold electron) resonance frequencies.
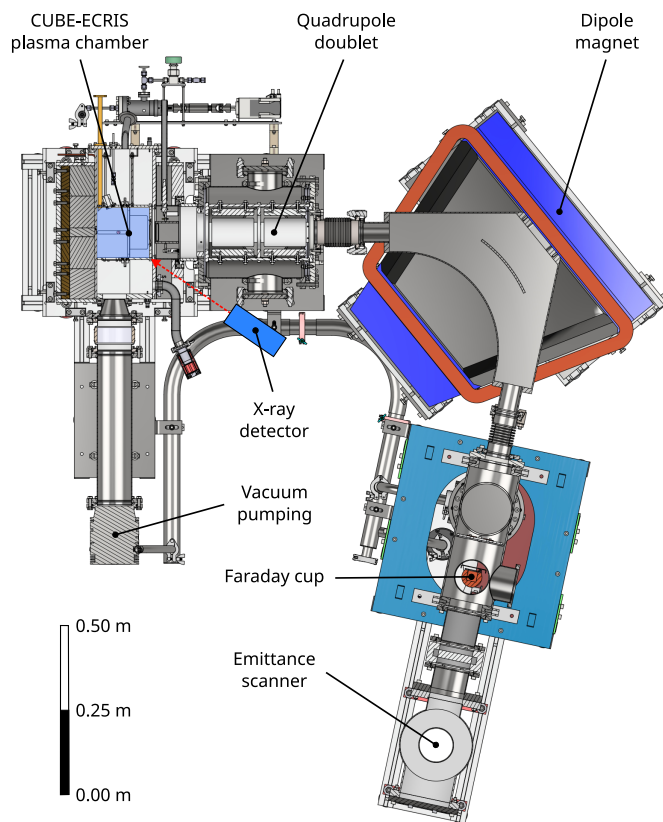

Fig. 3. The CUBE-ECRIS and low energy beam transport. The shown cross section corresponds to the central symmetry plane of the setup, which was used in the positioning of the x-ray detectors. The x-ray detector location indicated in the figure refers to both, the energy-resolving Amptek XR-100-CdTe x-ray detector, and the bismuth germanate x-ray scintillator. The Amptek detector line-of-sight is indicated with the red arrow.

even when the source parameters were varied and then returned back to their initial values in between consecutive data acquisitions. (ii) Second, the data acquisition time was chosen to be $20\,\mathrm{min}$ to acquire adequate statistics, which improves the accuracy of the spectral temperature fitting. (iii) Finally, the photon energy range $(60-160\,\mathrm{keV})$ for the spectral temperature fitting was chosen so that the R^2-value (regression coefficient) was always > 0.99. The exact value of the spectral temperature is affected if the fitting range is chosen to be excessively wide, i.e. if the the linear fit starts to deviate from the measured data. Based on the selected photon energy

range we estimate the uncertainty of the reported T_s-values to be $\pm 2\%$. This estimate was achieved by narrowing down the fitting range at the expense of reducing the statistics and observing the effect on the resulting T_s. The given uncertainty is such small that the corresponding confidence interval is not displayed in the data figures presented hereafter.

The m/q-analysed beam currents were measured from the Faraday cup. We used a mixture of argon and oxygen buffer gas to maximise the high charge state argon beam currents in all but one measurement as described below. Two charge state distributions (CSDs) were recorded for each set of ion source parameters, one in the beginning and another one at the end of each $1200\,\mathrm{s}$ bremsstrahlung measurement, to confirm that the ion source plasma conditions remained constant during the data acquisition. The source potential was kept constant at $10\,\mathrm{kV}$ while the negative puller electrode voltage (determining the electric field strength in the extraction gap together with the source potential) was $2.8-3.0\,\mathrm{kV}$. The electrostatic quadrupole voltages were optimised for the transport of Ar^{9+} beam. We note that the transport efficiency of the beams is estimated to be very modest, i.e. $<50\%$, owing to reasons outlined in Ref. [21].

The bremsstrahlung spectra and CSDs of the extracted beam were recorded as a function of various ion source parameters: (i) First, we varied the microwave power, provided by a Traveling-Wave Tube Amplifier (TWTA) by Xicom, in the range of $75-325\,\mathrm{W}$ (i.e. up to the maximum available power across the X-band frequencies). The reported microwave powers are the readings of a microwave diode detector connected to the output of the TWT amplifier via a directional coupler, i.e. the attenuation in the (short) transmission line is not accounted for. This does not affect the conclusions as we are interested in parametric trends, not absolute values of the absorbed power. (ii) We then swept the microwave frequency provided by a low-level signal generator (Keysight N5173B EXG X-series) from $10.3\,\mathrm{GHz}$ to $11.5\,\mathrm{GHz}$ and recorded the bremsstrahlung spectra and beam current CSDs at a number of "good" frequencies at which the high charge state currents reached a local maximum with $280\,\mathrm{W}$ power. The reflected power was less than $5\,\mathrm{W}$ in every measurement and, thus, the relative uncertainty of the reported microwave powers is estimated to be better than 2% (applicable to all microwave power values reported herafter). (iii) Next, we varied the argon gas feed rate keeping the oxygen valve closed and using $250\,\mathrm{W}$

microwave power at $10.96\,\mathrm{GHz}$. Changing the argon gas feed rate affects the neutral gas pressure and the total extracted current. Since the vacuum gauge measuring the ion source pressure is not connected directly to the plasma chamber, we consider the total current being a more representative (relative) measure of the gas feed rate effect. We adjusted the gas feed rate to achieve total currents of $0.96-1.32\,\mathrm{mA}$ (pressure gauge reading from low to high 10^{-6}) and recorded the bremsstrahlung and CSD data. (iv) We collected data in single (f_1) and dual ($f_1 + f_2$) frequency heating modes either matching the total power ($P_\Sigma = P_1 + P_2$) or the electric field (voltage) amplitude ($\sqrt{P_\Sigma} = \sqrt{P_1} + \sqrt{P_2}$) of the signals launched into the ion source. The two frequencies were provided by two identical low-level signal generators fed into the TWT amplifier via a co-axial combiner (such technique was first used in ECRIS context in Refs. [31] and [32]). The frequencies were selected by optimizing the high charge state production, and their respective powers were measured from the output of the TWTA switching off one of the frequency sources when recording the power at the other frequency. (v) Last, we measured the time-resolved bremsstrahlung power flux with the scintillator detector at $200-300\,\mathrm{W}$ microwave powers at $10.96\,\mathrm{GHz}$ frequency. This was done in order to probe the electron heating and confinement properties of the CUBE-ECRIS, and compare the plasma breakdown and decay times to those of conventional ECR ion sources.

IV. EXPERIMENTAL RESULTS

Figure 4 shows the bremsstrahlung spectra of the CUBE-ECR ion source recorded with several microwave powers in the $75-325\,\mathrm{W}$ range at $10.97\,\mathrm{GHz}$ frequency. The spectral temperature increases from $\sim30\,\mathrm{keV}$ to $\sim35\,\mathrm{keV}$ as the microwave power is increased across the given range.
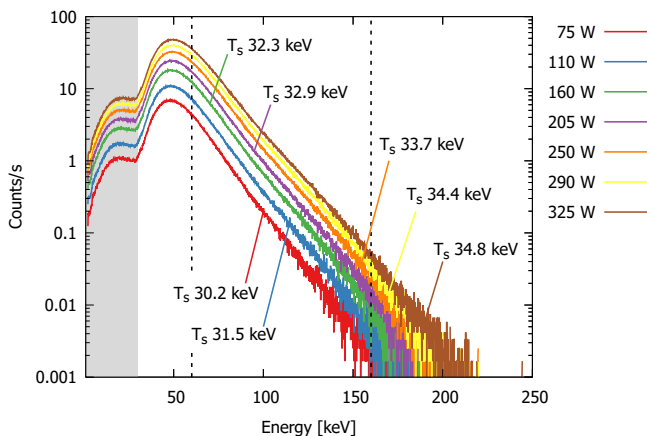
Fig. 4. The bremsstrahlung spectra (counts/second) of the CUBE-ECR ion source with microwave powers of $75-325\,\mathrm{W}$ at $10.97\,\mathrm{GHz}$ frequency. The total count rate increases linearly with the microwave power. The spectral temperatures T_s obtained from the slope of the linear fit in $60-160\,\mathrm{keV}$ energy range (bordered by the dashed lines) are indicated for each data set. The region with gray background at $\leq30\,\mathrm{keV}$ photon energies is where the attenuation in the mechanical structure of the ion source skews the spectrum.

The (normalized) bremsstrahlung count rate and high charge state argon ion currents, i.e. Ar^{8+}, Ar^{9+} and Ar^{11+}, as a
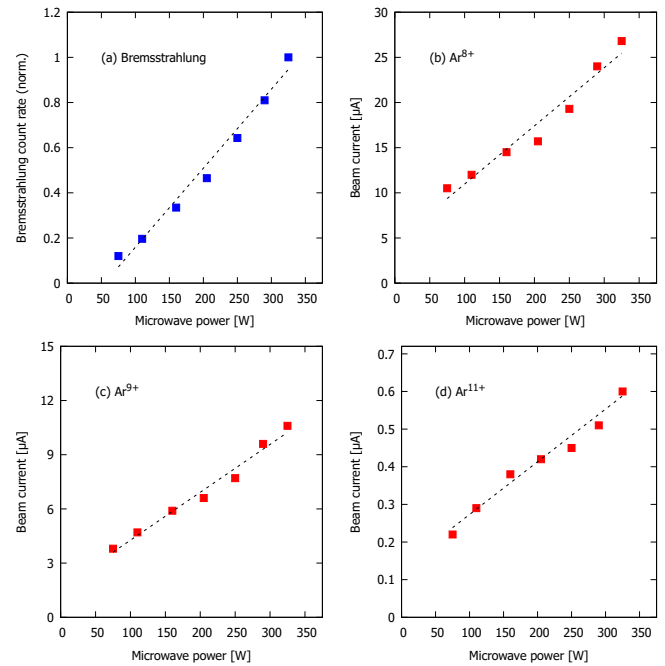

Fig. 5. The bremsstrahlung count rate (a) and Ar^{8+}, Ar^{9+} and Ar^{11+} beam currents (b)-(d) of the CUBE-ECR ion source as a function of the microwave power at $10.97\,\mathrm{GHz}$ frequency. The dashed lines are linear fits to the data to guide the eye.

function of the microwave power (at $10.97\,\mathrm{GHz}$) are shown in Fig. 5. All of them increase linearly with the microwave power, which indicates that the CUBE-ECR ion source operates below a saturation plasma energy content ($n_e < E_e >$, i.e. the product of the plasma density and average electron energy) when the gas feed rate is optimised for high charge state production. We have recently reported similar trend for record beams of krypton and xenon [33].

The bremsstrahlung spectra (counts/second) recorded during the frequency sweep in the range of $10.33-11.49\,\mathrm{GHz}$ (with $280\,\mathrm{W}$ power) are presented in Fig. 6. The spectral temperature remained virtually constant at $32-34\,\mathrm{keV}$ over this range at those frequencies deemed "good" as described in Section 3.
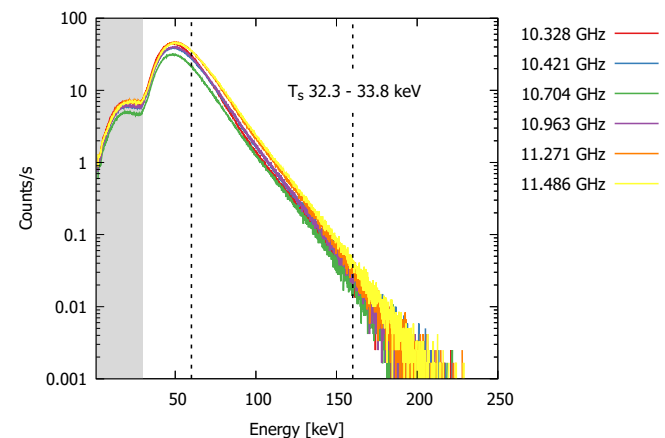

Fig. 6. The bremsstrahlung spectra (counts/second) of the CUBE-ECR ion source with microwave frequencies of $10.33-11.49\,\mathrm{GHz}$ with $280\,\mathrm{W}$ power.

The (normalized) bremsstrahlung count rate and high charge state argon ion currents recorded during the frequency sweep are shown in Fig. 7. There is no clear trend in the bremsstrahlung data nor in the currents of Ar^{8+} and Ar^{9+}. The beam current of the highest observed charge state, Ar^{11+}, increases almost monotonically with the microwave frequency up to approximately $11.3\,GHz$ and then collapses at higher frequencies. No "good" frequencies for high charge state production were found above this threshold, which is indicated by the dashed vertical line in Fig. 7(d). The reason for such behaviour is unknown. It is plausible that above $11.3\,GHz$ the CUBE-ECR operates with sub-optimal B-field mirror ratios, which limits the high charge state beam currents, or alternatively, the microwave-plasma coupling could be poor at frequencies exceeding this limit. We emphasise that the observation of poor performance above $11.3\,GHz$ is not based on the single data point presented in Fig. 7 but an extensive search (frequency sweep) of "good" frequencies up to $12\,GHz$ was conducted while bremsstrahlung data were taken above this threshold only at $11.49\,GHz$. The lack of an all-encompassing trend such as monotonic increase of the bremsstrahlung count rate and beam current (including a correlation between the two) with the frequency, which could be expected from the frequency scaling of the critical plasma density, and the seemingly random distribution of the "good" frequencies suggests that the source operates under critical density. In that case the microwave-plasma coupling and precise distribution of the microwave electric field in the loaded plasma chamber is important for the electron heating properties and high charge state beam performance of the ion source similar to most conventional Ku-band 2nd generation ECR ion sources (see e.g. Ref. [34] for a more precise frequency sweep).

Figure 8 shows the bremsstrahlung spectra of the CUBE-ECR ion source recorded with several total beam currents (argon feed rates) of $0.96-1.32\,mA$. The spectral temperature and the total count rate are independent of the gas feed rate. The charge state distribution of argon was observed to shift towards lower charge states with increasing pressure. We choose to refrain from presenting beam current data as no mixing gas was applied and, thus, the beam currents are far from optimum. Further details on the gas mixing effect in the CUBE-ECR can be found in Ref. [28].

Figure 9 summarizes the observed bremsstrahlung spectral temperatures as a function of the basic tuning parameters of the CUBE-ECRIS, namely microwave power, frequency and (argon) gas feed rate.

The bremsstrahlung spectra (counts/second) of the CUBE-ECR ion source with different frequency and power combinations in either single or dual frequency heating mode are shown in Fig. 10. The spectral temperature exhibits a weak dependence on the total power as noted above but is found independent of the plasma heating mode.

The corresponding x-ray count rates (normalized) and high charge state argon beam currents are listed in Table III. The beam currents of the highest charge states, e.g. Ar^{11+} can be optimised by applying microwave power at two frequencies $(250\,W + 80\,W)$. At the same time the total bremsstrahlung count rate is reduced in comparison to single frequency heating
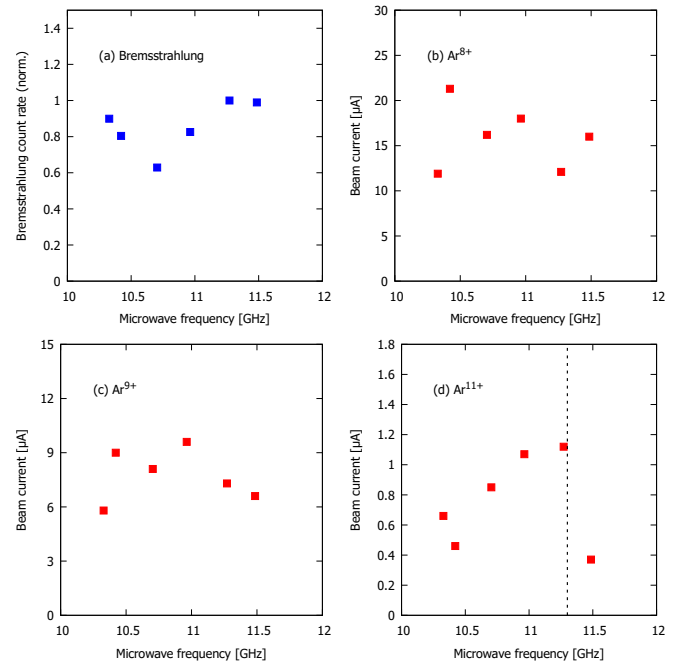

Fig. 7. The bremsstrahlung count rate (a) and Ar^{8+}, Ar^{9+} and Ar^{11+} beam currents (b)-(d) of the CUBE-ECR ion source as a function of the microwave frequency with $280\,W$ power. The dashed vertical line in (d) indicates the frequency of $11.30\,GHz$ above which the very high charge state output of the ion source collapses.
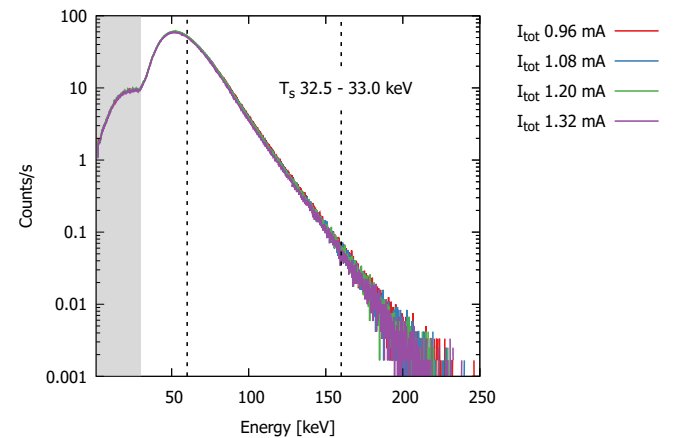

Fig. 8. The bremsstrahlung spectra (counts/second) of the CUBE-ECR ion source with total extracted currents of $0.96-1.32\,mA$ with $250\,W$ microwave power at $10.96\,GHz$ frequency. The total current was varied by changing the argon gas feed rate into the ion source.

with the same total power ($330\,W$), whereas the spectral temperature remains unchanged. In the third case shown in the table ($82\,W + 82\,W$) the maximum electric field amplitude of the combined signal equals the electric field amplitude E of the single frequency heating with $330\,W$ power ($E \propto \sqrt{P}$). Here the high charge state beam currents match those achieved in single frequency heating mode with significantly higher power. Single frequency heating with the same (approximate) total power of $160\,W$ yields lower beam current of the highest charge states but the same bremsstrahlung count rate.

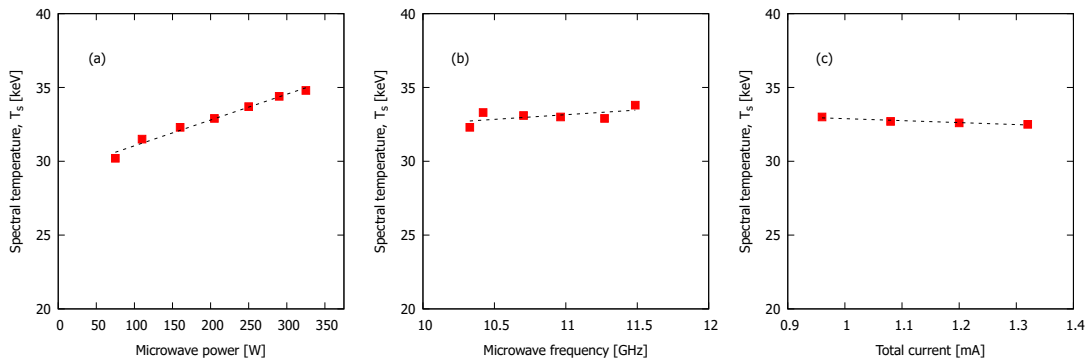The breakdown and decay transients of the bremsstrahlung

Fig. 9. The bremsstrahlung spectral temperature of the CUBE-ECR ion source as a function of (a) microwave power, (b) microwave frequency and (c) argon total current (gas feed rate). The dashed lines are to guide the eye.

TABLE III

THE BREMSSTRAHLUNG COUNT RATE AND HIGH CHARGE STATE ARGON BEAM CURRENTS WITH DIFFERENT FREQUENCY AND POWER COMBINATIONS.

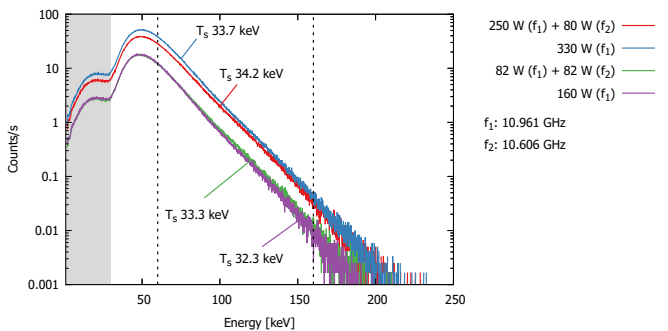| Frequency [GHz]	Power [W]	X-ray counts (norm.)	Ar^{8+} [μA]	Ar^{9+} [μA]	Ar^{11+} [μA]
10.961 + 10.606	250 + 80	0.74	19	9.9	1.2
10.961	330	1	19	9.0	0.7
10.961 + 10.606	82 + 82	0.31	14	6.9	0.7
10.961	160	0.31	15	6.0	0.4

Fig. 10. The bremsstrahlung spectra (counts/second) of the CUBE-ECR ion source with different frequency and power combinations in either single or dual frequency heating mode. The spectral temperatures T_s obtained from the slope of the linear fit in $60-160$ keV energy range (bordered by the dashed lines) are indicated for each data set.
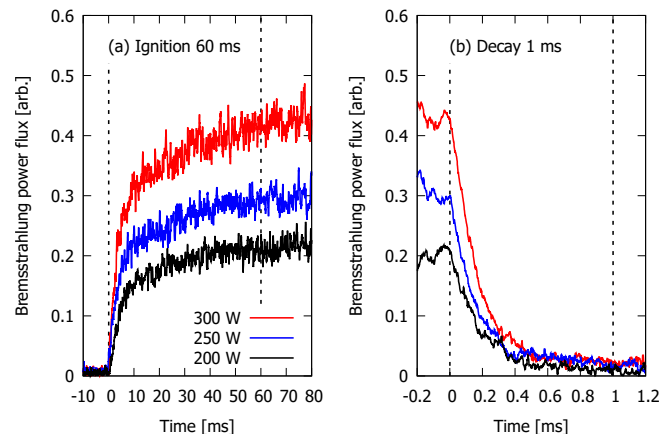

Fig. 11. The plasma breakdown and decay transients of the bremsstrahlung power flux of the CUBE-ECRIS with $200-300$ W microwave power at 10.96 GHz. The dashed lines represent the interval in which the bremsstrahlung power flux reaches / decays to 95% / 5% of its steady-state value with the plasma on / off.

power flux at three different microwave powers of $200-300$ W at 10.96 GHz are shown in Fig. 11. The duration of the breakdown transient to 95% of the saturation power flux is approximately 60 ms, independent of the microwave power. The decay transient is much faster; it takes only ~ 1 ms for the power flux to decrease to 5% of the saturation value. We note that the breakdown and decay transients are not linear but are best described by (nearly) logarithmic and exponential functions, respectively, until a saturation level is reached. Thus, the breakdown and decay times to reach $1/e$-thresholds of the saturation values (often regarded as the characteristic transient parameters) are shorter, approximately 8 ms and 0.2 ms, respectively.

V. DISCUSSION

The experimental results presented in Section IV corroborate the notion that, despite of the different magnetic field topology, the CUBE-ECRIS operates similarly to conventional ECR ion sources. The linear dependence of the bremsstahlung count rate and weak dependence of the spectral temperature on the applied microwave power are consistently observed with 2nd generation X- or Ku-band sources [25], [27]. Likewise, the neutral gas pressure does not have any effect on the bremsstrahlung emission characteristics in either source type. The implication is that the plasma hot electron density increases monotonically with the applied microwave power

whereas the electron energy distribution (inferred from the x-ray emission) appears to change only little. The monotonic increase of the hot electron density with microwave power has been observed earlier in quadrupole topology [22].

The fact that the microwave frequency does not have a systematic effect on the bremsstrahlung count rate or any effect on the spectral temperature rules out the $B_{\min}/B_{\mathrm{ECR}}$ or the mirror ratios $B_{\mathrm{wall}}/B_{\mathrm{ECR}}$ being the most important magnetic field parameter defining these emission characteristics, as concluded in Ref. [26] for conventional ECR ion sources. The same applies for the surface area of (and volume enclosed by) the ECR zone as well as the average field gradient at the resonance, which all increase notably with the microwave frequency, yet no systematic effect on the bremssstahlung count rate or any effect on the bremsstrahlung spectral temperature was found. Instead we find that our data points (quadrupole field) are very close those reported in Ref. [26] (solenoid + sextupole field) where the linear scaling of T_s with $B_{\min}$ was first observed. This is highlighted in Fig. 12 showing the data points of this study together with those from Ref. [26] in the $B_{\min}$-range of $0.1-0.5\,\mathrm{T}$. The cautious conclusion is that the $B_{\min}$-scaling of the bremsstrahlung T_s appears to be a fundamental property of minimum-B, high charge state ECR-heated plasmas with closed ECR-surface, not specific to the field topology. At the same time we acknowledge that, being a permanent magnet ion source, the CUBE-ECRIS provides only a single data point for the $B_{\min}$ and we might e.g. find a different slope of the linear dependence for the quadrupole field than observed for the superposition of the solenoid and sextupole fields.
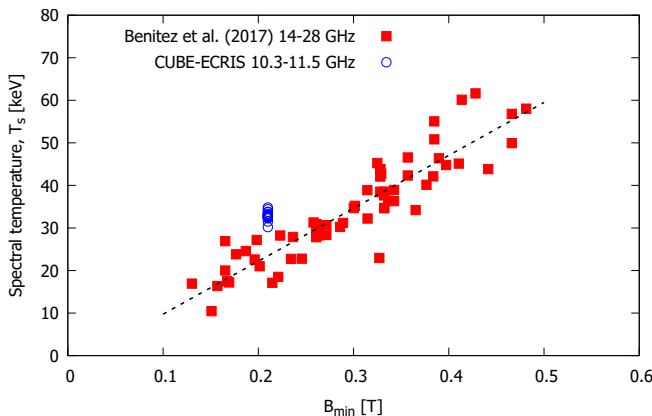

Fig. 12. The bremsstrahlung spectral temperature as a function of $B_{\min}$. The data from Benitez et al. [26] combines data (N=66) measured with 14, 18 and 28 GHz frequencies on conventional ECR ion sources and reveals the linear dependence of T_s on $B_{\min}$. The T_s-values measured with the minimum-B quadrupole CUBE-ECRIS (N=20) at 0.21 T $B_{\min}$ are close to those recorded with conventional ECRISs.

The data comparing the single and dual frequency heating modes reveals interesting tendencies. First and foremost, the bremsstrahlung spectral temperature is independent of the heating mode suggesting that the electron energy distribution is not affected by the partitioning of the power between the frequencies. On the other hand, we found that the bremsstrahlung count rate is lower when the production of high charge states

is optimise with dual frequency heating when comparing to single frequency data at the same total power. Furthermore it was observed that the same high charge state beam currents were achieved in single and dual frequency heating modes when the peak amplitudes of the microwave electric field (in the waveguide – not necessarily in the plasma chamber) were matched. It is possible that such trend is due to combining the frequencies at low power rather than launching them into the plasma chamber via two waveguide ports, which is the most usual configuration for dual frequency heating. The observation warrants further experiments with conventional ECR ion sources where different power combining schemes can be readily studied.

The time-resolved bremsstrahlung measurements reveal that the plasma breakdown transient of the CUBE-ECRIS is slightly faster than the breakdown transient of a conventional 2nd generation A-ECR type ECRIS where the bremsstrahlung emission saturates in $200-500\,\mathrm{ms}$ [35], [36]. This implies that the electron heating properties are rather similar between the two differing magnetic topologies. On the contrary, the $\sim 1\,\mathrm{ms}$ decay transient of the CUBE-ECRIS is two orders of magnitude faster than the $\sim 100\,\mathrm{ms}$ decay transient of the conventional ECRIS [37], which suggests that the electron confinement in the quadrupole minimum-B field is weaker. The suboptimal confinement of high energy electrons is likely to contribute to the difference between the high charge state currents of the CUBE-ECRIS and the best performing permanent magnet ion sources (see a review in Ref. [23]), along with the modest beam transport efficiency [21].

Overall, the bremsstrahlung experiments reassert the perception that there is no fundamental difference between quadrupole minimum-B ECR ion sources and conventional ECR ion sources in terms of electron heating. It is expected that the bremsstrahlung maximum energy and spectral temperature scale with $B_{\min}$ if the magnetic field and plasma heating frequency are increased. As such, the results support further development of the ARC-ECRIS concept towards higher frequencies. At the same time the rather modest high charge state ion currents (see Figs. 5 and 7) and weaker electron confinement (inferred from the decay transient in Fig. 11) highlight the importance of further prototyping with room-temperature devices in $10\text{-}18\,\mathrm{GHz}$ frequency range, including beam transport, before proposing a detailed design of a superconducting version of the quadrupole minimum-B ECRIS.

DATA AVAILABILITY STATEMENT

ACKNOWLEDGMENT

REFERENCES

[1] R. Geller, IEEE Transactions on Nuclear Science, vol. 26, no. 2, pp. 2119-2127, April 1979.

[2] C. Lyneis, Operating experience with the LBL ECR source Int. Conf. on ECR Ion Sources and their Applications (East Lansing, MI) ed J Parker pp 42-56, 1987.

[3] B. Jacquot, M. Pontonnier, Nucl. Instrum. Meth. A 287 (1990) 341–347.

[4] C. M. Lyneis, Z. Xie, D. J. Clark, R. S. Lam, S. A. Lundgren, Proceedings of the 10th International Workshop on ECR Ion Sources, Knoxville, USA, 1990, pp. 47–62.

[5] T. Kalvas, H. Koivisto and O. Tarvainen, AIP Conf. Proc. 2011, 040006 (2018).

[6] P. A. Zavodszky et. al., Rev. Sci. Instrum., 79, 02A302, (2008).

[7] D. Leitner, C. M. Lyneis, T. Loew, D. S. Todd, S. Virostek and O. Tarvainen, Rev. Sci. Instrum. 77, 03A302 (2006).

[8] L. Sun *et al*. 2020 Rev. Sci. Instrum. 91 023310.

[9] L. Sun *et al*., Proceedings of the 24th International Workshop on ECR Ion Source (ECRIS 2020), Published in: JACoW ECRIS2020 (2022) MOWZO01.

[10] D. Xie, J. Benitez and D. Todd, 2022 J. Phys.: Conf. Ser. 2244 012015.

[11] T. Antaya and S. Gammino, Rev. Sci. Instrum. 65, 1723 (1994).

[12] D. Hitz, A. Girard, G. Melin, S. Gammino, G. Ciavola and L. Celona, Rev. Sci. Instrum. 73, 509 (2002).

[13] C. Lyneis, P. Ferracin, S. Caspi, A. Hodgkinson, and G. L. Sabbi, Rev. Sci. Instrum. 83, 02A301 (2012).

[14] T. Lamy *et al*., in Proceedings, 13th Heavy Ion Accelerator Technology Conference (HIAT2015) : Yokohama, Japan, September 7-11, 2015, jacow.org

[15] V. Skalyga, I. Izotov, S. Golubev, A. Sidorov, S. Razin, A. Vodopyanov, O. Tarvainen, H. Koivisto and T. Kalvas, Rev. Sci. Instrum. 87, 02A716 (2016).

[16] G. D. Porter and M. Rensink, J. Vac. Sci. Technol. A 3, 1157 (1985).

[17] M. Inutake, T. Cho, M. Ichimura, K. Ishii, A. Itakura, I. Katanuma, et al., Phys. Rev. Lett. 55, 939 (1985).

[18] C. C. Petty, D. K. Smith, and D. L. Smatlak, Rev. Sci. Instrum. 59, 601 (1988).

[19] P. Suominen and F. Wenander, Rev. Sci. Instrum. 79, 02A305 (2008).

[20] P. Suominen, T. Ropponen and H. Koivisto, Nucl. Instrum. Meth. A 578, 370 (2007).

[21] S. Kosonen, T. Kalvas, H. Koivisto, O. Tarvainen and V. Toivanen, "Slit extraction and emittance results of a permanent magnet minimum-B quadrupole electron cyclotron resonance ion source", Nucl. Instrum. Meth. B, Volume 546, 2024, 165147.

[22] A. Girard, P. Briand, G. Gaudart, J. P. Klein, F. Bourg, J. Debernardi, J. M. Mathonnet, G. Melin, and Y. Su, Rev. Sci. Instrum. 65, 1714 (1994).

[23] T. Kalvas, V. Toivanen, H. Koivisto and O. Tarvainen, 2020 JINST 15 P06016.

[24] T. Thuillier, J. Benitez, S. Biri and R. Rácz, Rev. Sci. Instrum. 93, 021102 (2022).

[25] B. S. Bhaskar, H. Koivisto, O. Tarvainen, T. Thuillier, V. Toivanen, T. Kalvas, I. Izotov, V. Skalyga, R. Kronholm, and M. Marttinen, Plasma Phys. Controlled Fusion 63, 095010 (2021).

[26] J. Benitez, C. Lyneis, L. Phair, D. Todd, and D. Xie, IEEE Trans. Plasma Sci. 45, 1746–1754 (2017).

[27] J. Noland, J. Y. Benitez, D. Leitner, C. Lyneis, and J. Verboncoeur, Rev. Sci. Instrum. 81, 02A308 (2010).

[28] V. Toivanen, T. Kalvas, H. Koivisto, S. Kosonen and O. Tarvainen, "Gas mixing and double frequency operation of the permanent magnet qaudrupole minimum-B electron cyclotron resonance ion source CUBE-ECRIS", submitted to IoP Journal of Physics; Conference Series, (2023).

[29] T. Kalvas, V. Toivanen, S. T. Kosonen, H. Koivisto, O. Tarvainen and L. Maunoury, 2022 Plasma Sources Sci. Technol. 31 12LT02.

[30] M. Marttinen, B. Bhaskar, T. Kalvas, H. Koivisto, S. Kosonen, R. Kronholm, A. Ikonen, O. Tarvainen, O. Timonen, V. Toivanen, I. Izotov, V. Skalyga, J. Angot, T. Thuillier and L. Maunoury, Proc. ECRIS2020, doi:10.18429/JACoW-ECRIS2020-TUZZO02, (2020).

[31] R. C. Vondrasek, R. Scott and R. C. Pardo, Review of Scientific Instruments 77, 03A337 (2006).

[32] H. Koivisto, P. Suominen, O. Tarvainen, A. Virtanen and A. Parkkinen, Review of Scientific Instruments 77, 03A316 (2006).

[33] O. Tarvainen, D. Faircloth, J. Julin, T. Kalvas, H. Koivisto, S. Kosonen and V. Toivanen, "Permanent magnet ECR ion source and LEBT dipole for single-ended heavy ion ToF-ERDA facility", submitted to IoP Journal of Physics; Conference Series, (2023).

[34] F. Maimone, K. Tinschert, P. Spädtke, J.Mäder, J. Roßbach, R. Lang and L. Celona, Proc. ECRIS2010, Grenoble, France, TUPOT012, jacow.org, available online at https://accelconf.web.cern.ch/ECRIS2010/papers/tupot012.pdf

[35] T. Ropponen, O. Tarvainen, P. Jones, P. Peura, T. Kalvas, P. Suominen, H. Koivisto and J. Ärje, Nucl. Instr. and Meth. A 600, 525 (2009).

[36] T. Ropponen, O. Tarvainen, P. Jones, P. Peura, T. Kalvas, P. Suominen and H. Koivisto, IEEE Trans. Plasma Sci. 37, 2146 (2009).

[37] O Tarvainen et al 2010 Plasma Sources Sci. Technol. 19 045027.

Olli Tarvainen Olli Tarvainen was born in Joensuu, Finland, in 1979. He received his Ph.D. degree in physics from the University of Jyväskylä, Finland, in 2005. He then joined Los Alamos National Laboratory, NM, USA, as a postdoctoral researcher before returning to University of Jyväskylä in 2009 where he worked as a university researcher and lecturer. He joined the ISIS Neutron and Muon source at the Rutherford Appleton Laboratory of the UK Science and Technology Facilities Council in 2018, and is currently the leader of the low energy beam physics section. His main research interests are plasma physics and diagnostics of positive and negative ion sources, and applications of ion sources and low temperature plasmas.

Ville Toivanen Ville Toivanen was born in Rautavaara, Finland, in 1984. He received his Ph.D. degree in physics from the University of Jyväskylä, Finland, in 2013. After that he worked as a postdoctoral fellow at European Organization for Nuclear Research (CERN), Geneva, Switzerland, and as a postdoctoral researched at Grand Accélérateur National d'Ions Lourds (GANIL), Caen, France, before returning back to the University of Jyväskylä in 2018, where he currently works as a Staff Scientist. His main research interests include ion source technology and production of highly charged ion beams.

Taneli Kalvas Taneli Kalvas was born in Tampere, Finland, in 1981. He received his Ph.D. degree in accelerator/ion source physics from the University of Jyväskylä, Finland, in 2013, where he is currently working as a Staff Scientist. His main research interests are in numerical modeling of ion optics and plasma extraction and the applications of ion sources and accelerator technology. He manages the technical operations of the Accelerator Laboratory at the University of Jyväskylä.

Hannu Koivisto Hannu A. Koivisto was born in Alajärvi, Finland. He received the Ph.D. degree in physics from the Department of Physics, University of Jyväskylä (JYFL), Jyväskylä, Finland, in 1998. In 1998–1999, he had a Postdoctoral position with NSCL/MSU. He then returned to his home laboratory, where he is presently the Leader of the Ion Source Group of the Department of Physics, JYFL. The main research work has been done for developing the MIVOC method, designing and constructing ECR ion sources, developing metal ion-beam production, studying the ECR heated plasma and ion-beam production.

Sami Kosonen Sami Kosonen was born in Savonlinna, Finland, in 1988. He received his M.Sc. Degree in physics from the Department of Physics, University of Jyväskylä, Jyväskylä Finland, where he is currently working toward the Ph.D. degree in the Ion Source Group. His main research interests are numerical modelling and experimental work on plasma extraction, especially focusing on the the applicability of Child-Langmuir law in plasma ion source extraction systems.